

Supporting Information Appendix

Adaptive evolution of genomically recoded *Escherichia coli*

Timothy M. Wannier^{1†}, Aditya M. Kunjapur^{1†}, Daniel P. Rice², Michael J. McDonald², Michael M. Desai², George M. Church^{1*}

1 Department of Genetics, Harvard Medical School, 77 Avenue Louis Pasteur, NRB 238, Boston, MA 02115

2 Department of Organismic and Evolutionary Biology, Harvard University, 457 Northwest Labs, 52 Oxford Street, Cambridge, MA 02138

† These authors contributed equally to this work.

* Corresponding author: George M. Church, 77 Avenue Louis Pasteur, NRB 238, Boston, MA 02115, 617-432-7562, gchurch@genetics.med.harvard.edu

SI Discussion

Mutations found to broadly affect all evolved populations

We identified genes mutated multiple times across independent populations as putative targets of selection. For each lineage and for all lineages combined, we compared the distribution of the number of independent mutations observed per gene to the expectation under multinomial resampling (**Fig. S9**). In each comparison, the observed distribution has a much heavier right tail than the expected distribution, indicating enrichment in multiply mutated genes. Table S3 lists the 50 genes with at least four independent mutations in any lineage or at least six mutations across all lineages, while Table 1 lists a subset of these that are of interests to the discussion in this work. Many of these genes are common genetic targets in previous ALE studies or have been noted as being adaptive to minimal media or biofilm formation. In particular, 10 of these 50 genes were found previously during adaptive evolution of *E. coli* K-12 strains to minimal media. These include *pykF*, *rph*, *rpoB*, and *rpoC*, found in three studies from the Palsson laboratory (1–3); *fis*, *gltB*, *kup*, and again *pykF* found by the Lenski laboratory (4); *fimH* found by a Bolívar lab study (5), and *folA* found during C321 passaging by the Barrick Lab (6).

It has been previously documented that a frameshift mutation in the C-terminus of *rph* in wild-type K-12 strains causes pyrimidine starvation in minimal media. This is due to low *pyrE* expression because a premature *rph* stop codon impedes transcription/translation coupling, which supports optimal levels of *pyrE* expression past the intercistronic *pyrE* attenuator (7). Evolutionary studies from the Palsson lab identified a recurring 82-bp deletion in the regulatory region between *rph* and *pyrE*. In contrast, we in no cases see this same deletion, but instead see thirteen separate mutations to a 233-bp stretch extending from the C-terminus of *rph* through some intergenic space, and into the first 15-bp of the *pyrE* gene. The five most frequent mutations make up 86% of the total hits. Four of these are in the first attenuator stem, weakening it (**Fig. S10**), and the other, found in eight clonal isolates from four populations, is an exact reversion (3815879 TCC to TCCC) to restore the original wild-type locus found in the K-12 ancestor. Other mutations found are frameshifts in *rph* to extend its reading frame either by 10 amino acids to its wild-type UGA or a further 14 amino acids to a UAG stop codon, which we presume also relieves *pyrE* attenuation.

Of the other genes that we found in common with previous ALE studies, mutations to RNA polymerase subunits B and C (*rpoB* and *rpoC*) have been particularly well-documented. In one study, Conrad *et al.* characterized three *rpoB* mutations that were found during ALE to glucose minimal media, and determined that all variants were fitter in defined media, but less fit in rich media (1). Conrad *et al.* additionally found that these variants exhibited decreased open-complex longevity and greater processivity, which they proposed led to greater expression of metabolic genes, and lower rRNA expression. In this work we found eleven unique *rpoB* variants and 20 unique *rpoC* variants, all of which are mis-sense mutations, and none of which were documented in previous ALE studies. This suggests to us that the landscape for adaptive fitness gain in the two polymerase subunits is quite large, with many routes to switching between adaptation to LB and glucose minimal media.

Eight of the remaining 43 genes, including many of the most heavily-mutated genes, are involved in biofilm formation. A study by Danese *et al.* showed that gene *flu* (or *agn43*) is an abundant outer-membrane protein that is important for biofilm formation in glucose minimal media but not in rich media (8). The same study demonstrated that *fimH* is important for biofilm formation in both poor and rich media and showed the role of *oxyR* as a repressor of *flu*. A gene expression study found that *gltB* and *ompT* were expressed at levels 12- and 39-fold higher levels in biofilm growth compared to stationary phase (9). Purine biosynthesis has been shown to be important for biofilm formation in *E. coli* and other Gram-negative bacteria, with a study in *Burkholderia* specifically implicating *purL* and *purT*. Finally, *mdtJ* null strains were shown to have enhanced biofilm growth (10).

Differences in stop codon effectiveness at translation termination

The effectiveness of stop codons at coding for translation termination is affected by their identity (UAG, UGA, or UAA) and by sequence context (11–13). Suppression experiments suggest that UAA codons, which are recognized by both RF1 and RF2, are read more often by RF1 in *E. coli* K12 (14). Analyses in *E. coli* show that codon adaption index correlates positively with increasing UAA preference (15) and that most highly expressed genes end in UAA (16). In the absence of RF1, insufficient RF2 activity in C321.ΔA strains may impair fitness due to ribosome stalling at UAA or UGA stop codons. This would result in a smaller pool of free ribosomes, lower translational capacity, and increase the requirement for ribosome rescue by tmRNA-mediated trans-translation (17, 18) or by alternative ribosome-rescue factor (19, 20).

Previous observations of *prfB* and *prfC* mutations resulting from defective translation termination at the ribosomal level

Mutations to *prfB* and *prfC* also occur in response to translation termination impairment at the ribosomal level, especially where interactions occur with RFs. 23S ribosomal RNA (rRNA) is modified by the pseudouridine synthase RluD at positions that form a bridge between the 20S and 50S ribosomal subunits and interact with translation factors and tRNAs throughout protein synthesis (21–23). In $\Delta rluD$ K-12 strains, suppressor-containing derivatives rapidly arose from slow growing cultures (22, 23). One study identified and characterized one suppressor strain containing PrfB_E172K and found that wild-type levels of termination were restored at UAA codons after *rluD* inactivation (22). Another study investigated 21 additional suppressor strains (23). Of these strains, 15 contained point mutations in *prfB* (resulting in amino acid changes of D131Y, E157K, E167K, E172A, Q290K, A293T, and A293V) and 5 contained point mutations in *prfC* (T30I, T99I, V119F, V119G, and D313Y). Interestingly, none of these positions were found to be effected in our adaptive evolution study. However, deliberate replacement of the K-12 *prfB* gene with the *E. coli* B *prfB* (PrfB_T246A) and subsequent inactivation of *rluD* resulted in negligible impairment to growth and translation termination (23).

Effect of media composition on strains containing release factor mutations

Minimal media can enhance the severity of release factor mutations. One set of investigations found that PrmC (an N^5 -glutamine methyltransferase that enhances the activity of RF1 and RF2) inactivation in *E. coli* imparts growth defects, particularly in minimal media or with poorer carbon sources, due in part to translational read-through of stop codons (24–26).

Strategies to improve protein expression in evolved recoded strains

Our data indicate that recoded strain capacity for protein overproduction in glycerol minimal media was significantly impaired, but that ALE here restored this deficit. Evolution for successive passaging fitness, should however not have selected for protein production, but for improved growth rate, and therefore we believe that rational genome engineering can be used to further improve protein expression in these strains. Well-documented targets include proteases encoded by *lon* (27) and *ompT* (28), as well as nucleases encoded by *rnb* (29), *rne* (30), and *endA* (31).

Others have attempted to engineer some of these targets in C321.ΔA and observed increased protein expression (32). While the expression of nsAA-containing proteins may also benefit from these approaches, nsAA incorporation faces other limitations that ought to be addressed, such as limited activity and selectivity in the engineered orthogonal aminoacyl-tRNA synthetases. An unusually selective but not highly active synthetase was used for nsAA incorporation in this study. Rational engineering or directed evolution approaches can be used to generate synthetases with improved attributes in either or both categories.

SI Figures

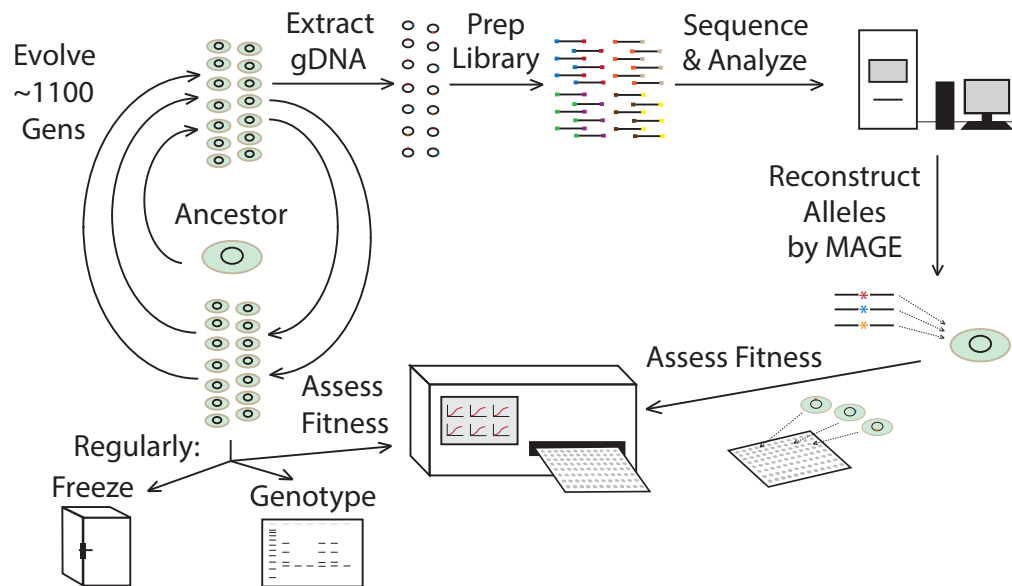


Figure S1. Project workflow for long-term adaptive laboratory evolution (ALE) of recoded *Escherichia coli*. Briefly, strains were passaged in serial batch cultures as 14 independent replicates for 1,000+ generations with routine genotyping (via allele-specific PCR and gel electrophoresis), storage as glycerol stocks, and growth rate analysis by plate reader. Two clones from each population at the final time point were used for genomic DNA preparation and Illumina sequencing library preparation. Sequencing was performed, data was analyzed to identify variants, and MAGE was used to reconstruct alleles in ancestral strains.

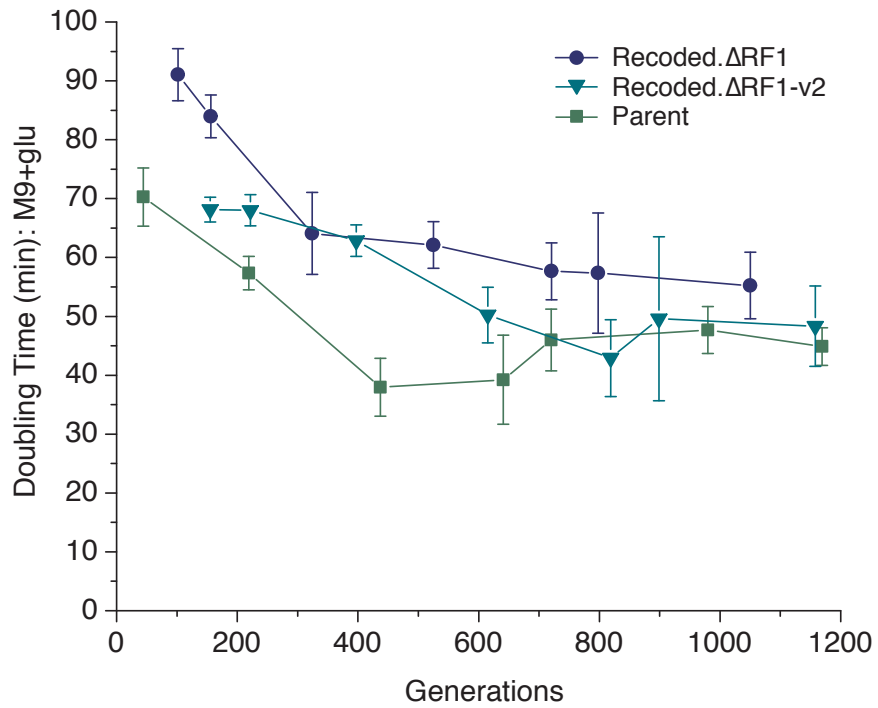


Figure S2. Trajectories of strain doubling time as a function of generation during evolution. This data was obtained by sampling individual colonies from all 14 replicate populations for each strain.

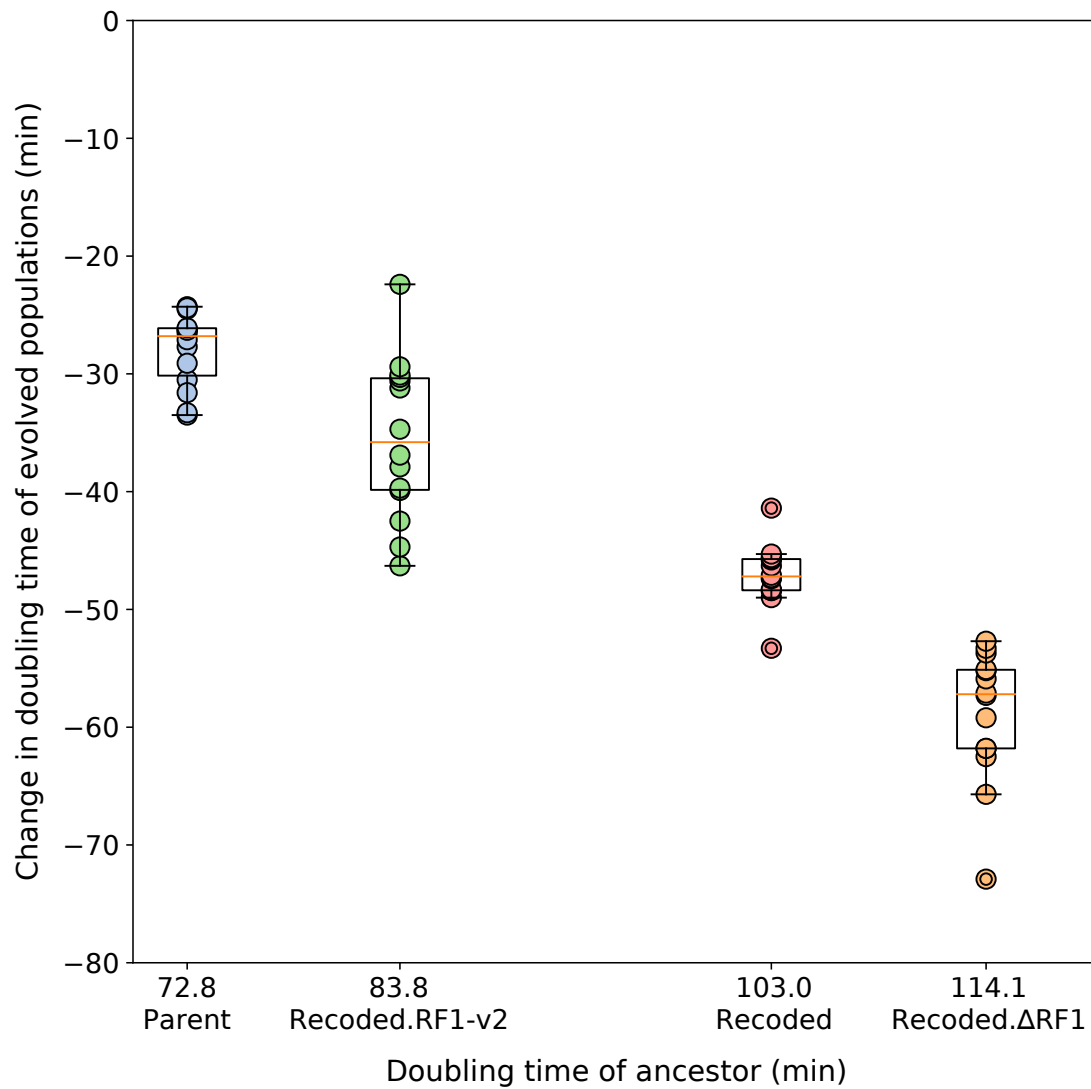


Figure S3. The change in doubling time of evolved populations in M9 + 1% glucose inversely correlates with the doubling time of the variants' ancestors.

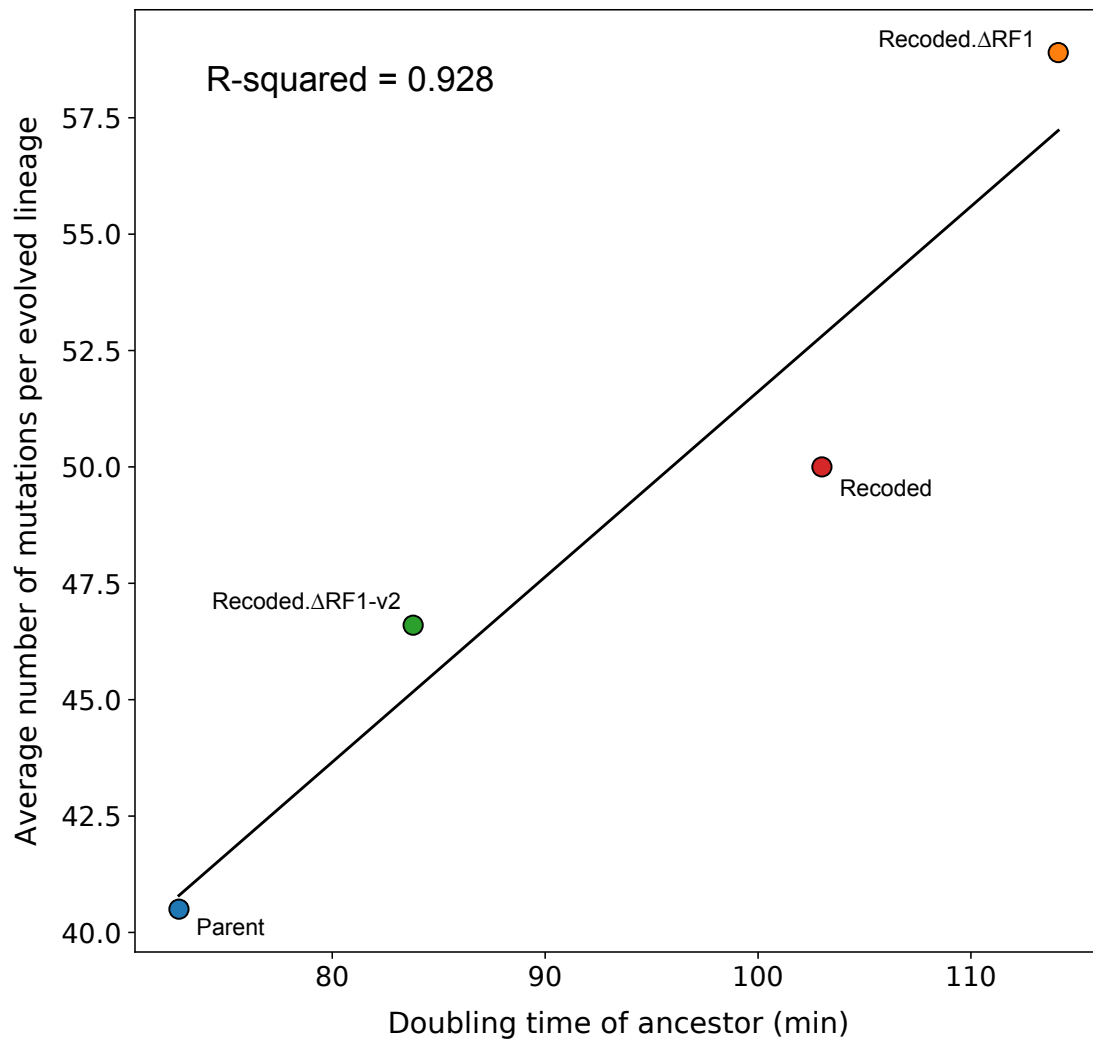


Figure S4. Relationship between the doubling time of the ancestral strain and the average number of mutations incorporated in the evolved lineages.

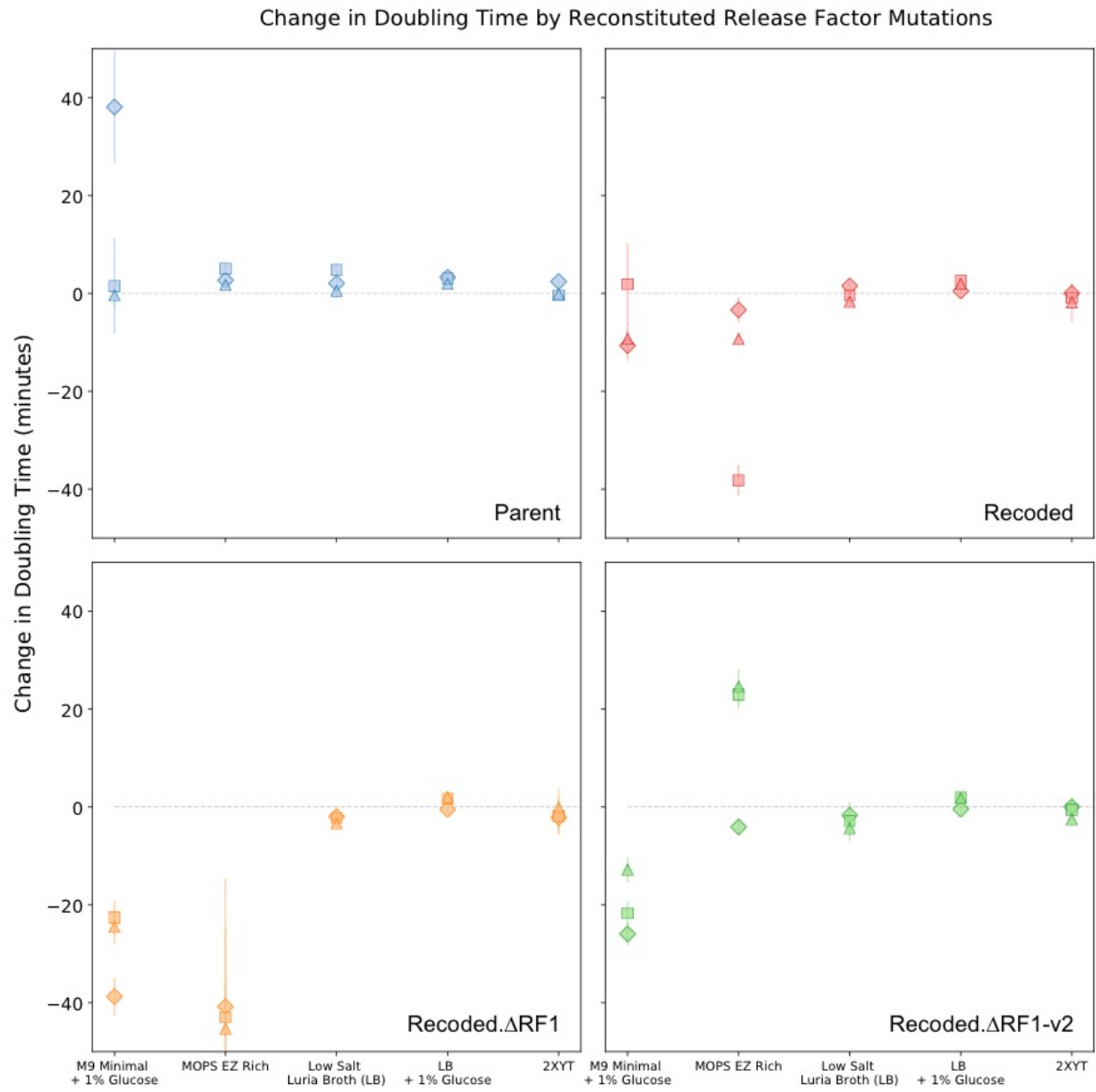


Figure S5. Change in the doubling time of ancestral lineages with various RF mutations in five different media.

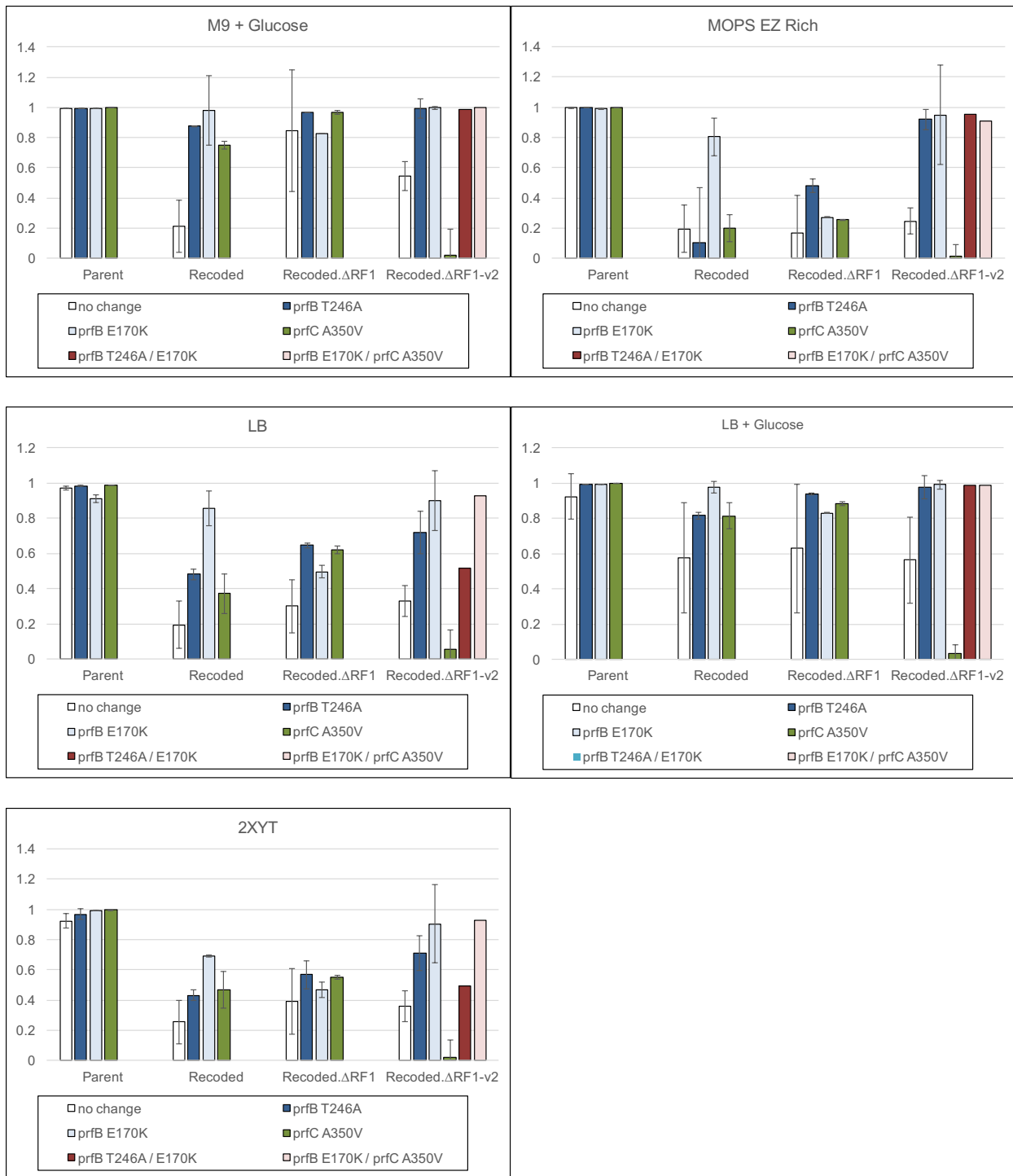


Figure S6. Results from a competition assay of strains containing release factor variants. The percentages in the figure indicate the percent of cells that were non-fluorescent after a 24-hour head-to-head competition, in which each strain was competed against a fluorescent reference strain. These measurements were made in triplicate.

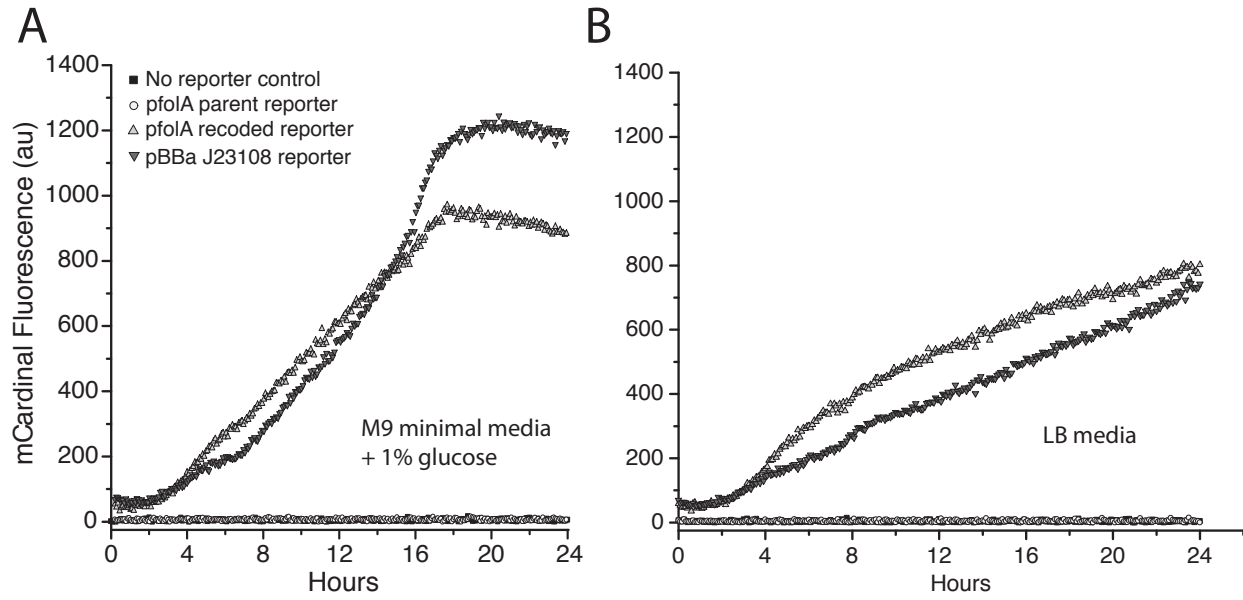


Figure S7. Effect of the *foIA* promoter mutation on fluorescence resulting from fluorescent protein gene expression in (A) M9 minimal media + 1% glucose or (B) LB media.

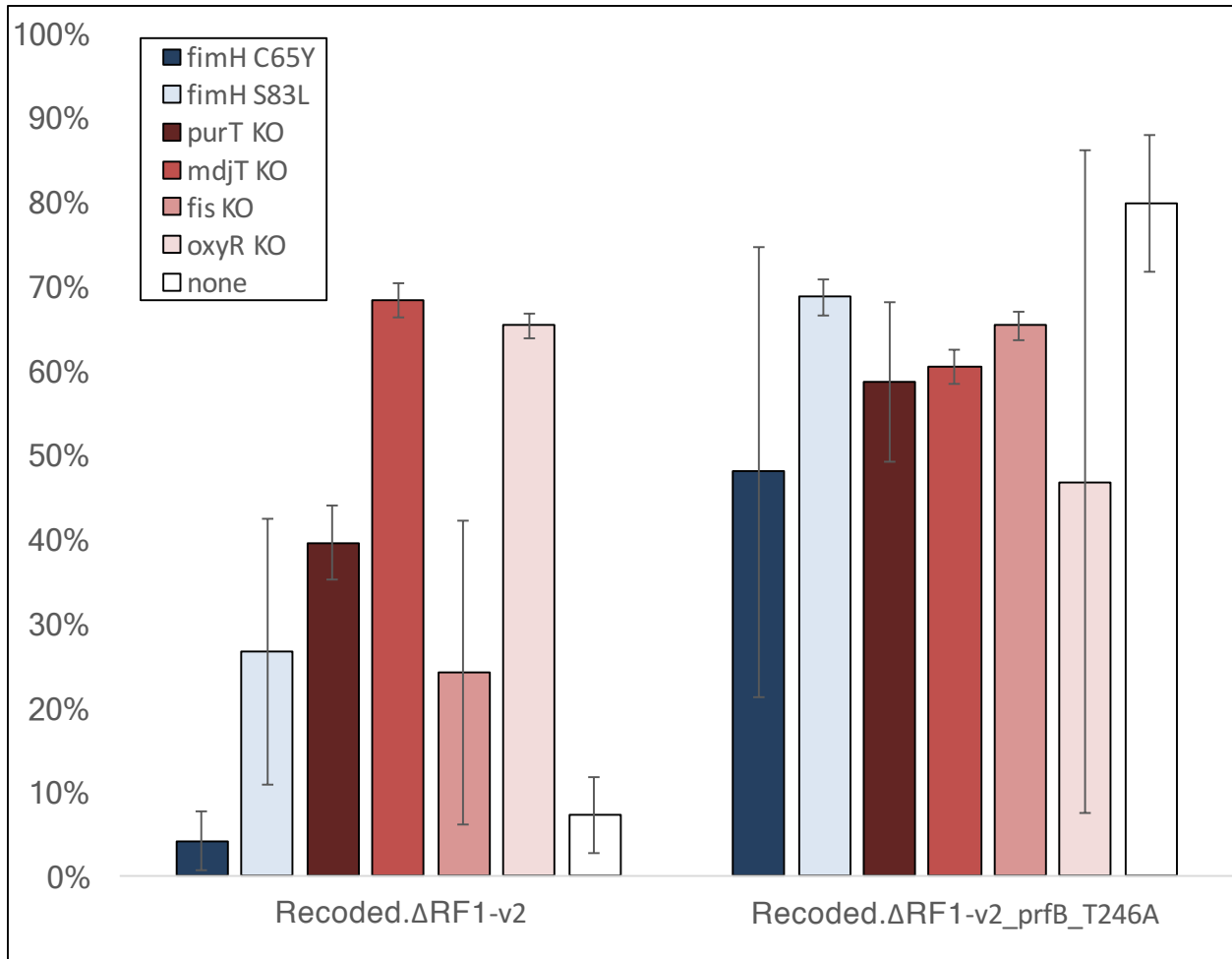


Figure S8. Head to head competition assay results for strains containing other mutations of interest. The percentages in the figure indicate the percent of cells that were non-fluorescent after a 24-hour head-to-head competition, in which each strain was competed against a fluorescent reference strain. These measurements were made in triplicate.

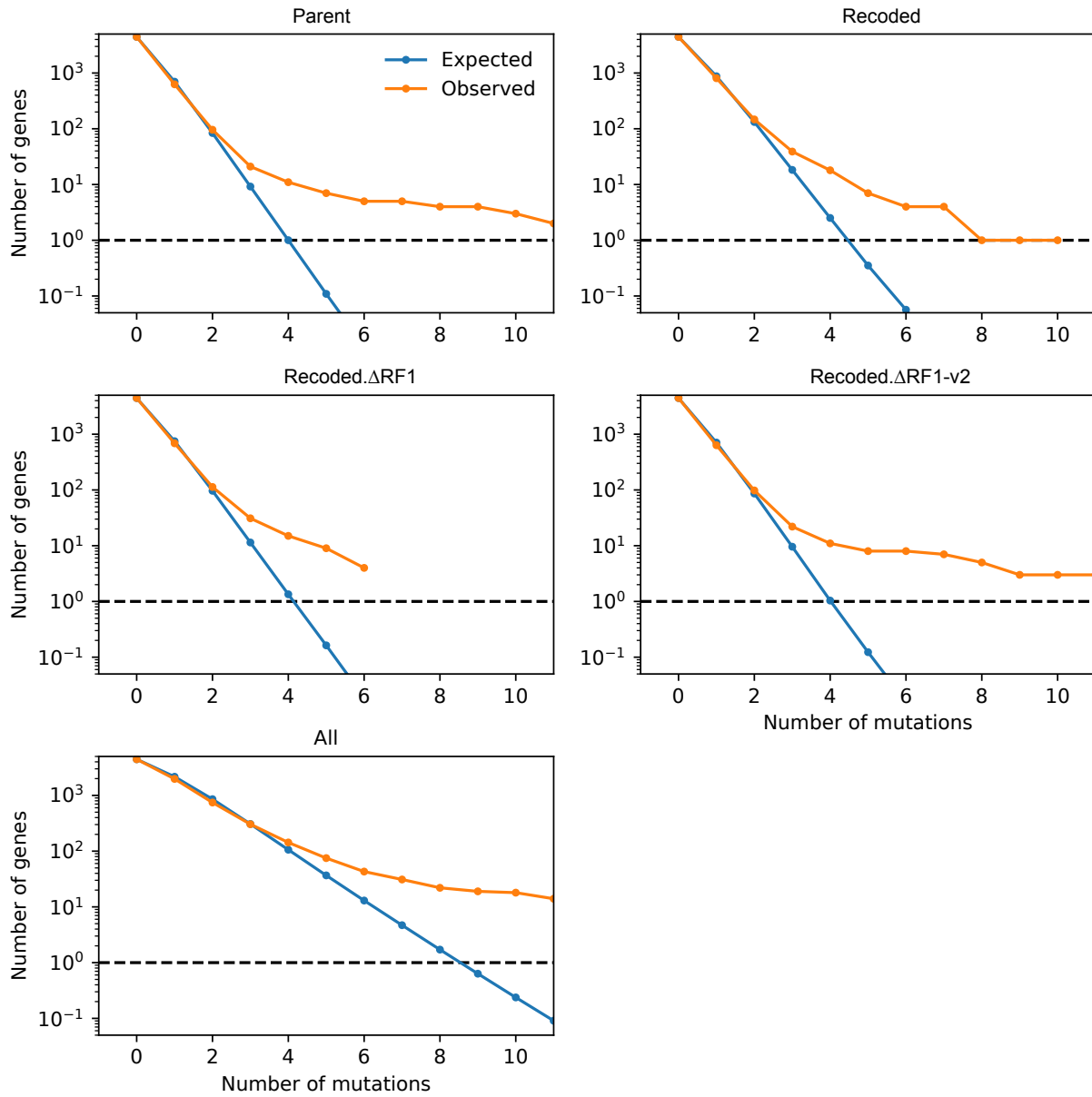
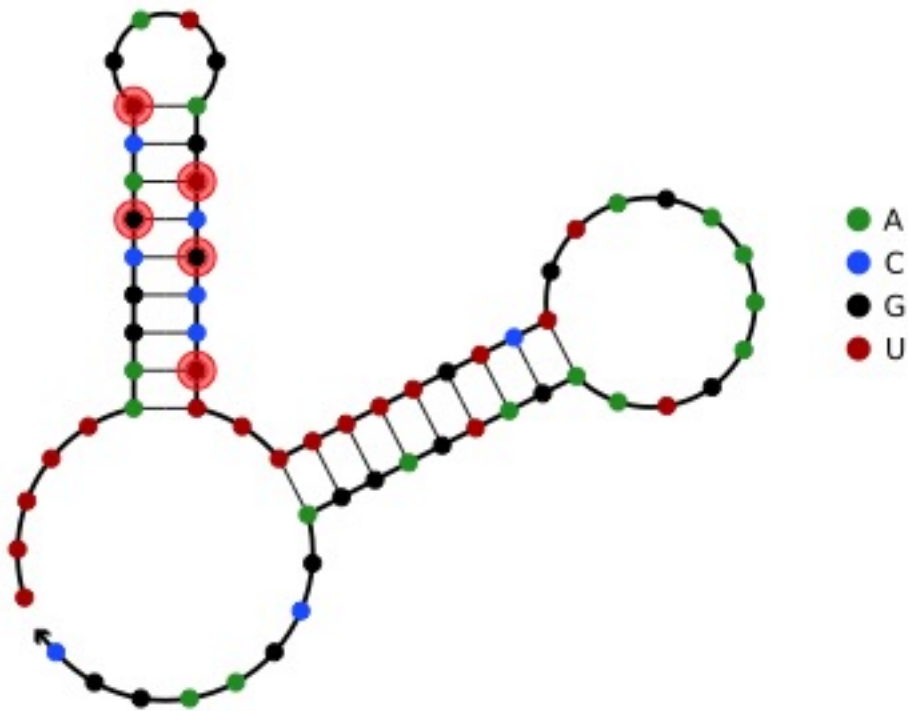


Figure S9. Complementary cumulative distributions of the number of mutations per gene. The orange curves show the number of genes in which we observed at least n independent mutations at generation 1,100 as a function of n , within each lineage and across all populations. The blue curves show the average of 10,000 multinomial re-samplings with the total number of mutations fixed and expected number of mutations per gene proportional to gene length.

MFE structure at 37.0 C



Free energy of secondary structure: -19.20 kcal/mol

Figure S10. Predicted secondary structure of the attenuator loop between *rph* and *pyrE*. Sites that were observed to mutate in the evolved populations are highlighted in red. Nupack was used to simulate the RNA structure at 37°C in normal physiological conditions.

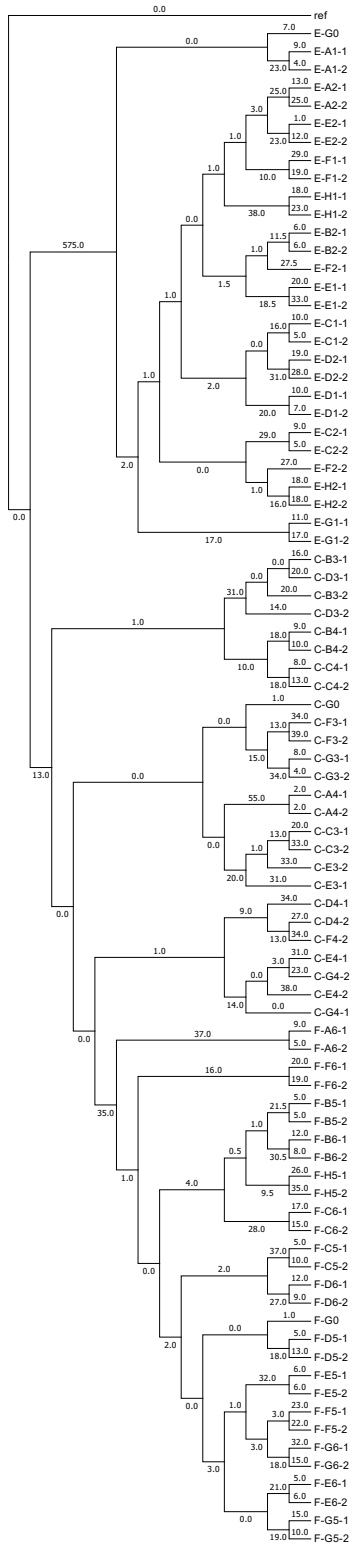


Figure S11. Maximum parsimony phylogenetic tree detailing all potential well-well cross-seeding events.

SI Materials and Methods

Culture Conditions:

A 1X M9 salt medium (M9+glucose) containing 6.78 g/L $\text{Na}_2\text{HPO}_4 \cdot 7\text{H}_2\text{O}$, 3 g/L KH_2PO_4 , 1 g/L NH_4Cl , and 0.5 g/L NaCl, supplemented with 1 mM MgSO_4 , 0.1 mM CaCl_2 , 1% glucose, trace elements, biotin, and carbenicillin was used as the culture medium for evolution and most experiments in this study. The trace element solution (100X) used contained 5 g/L EDTA, 0.83 g/L $\text{FeCl}_3 \cdot 6\text{H}_2\text{O}$, 84 mg/L ZnCl_2 , 10 mg/L $\text{CoCl}_2 \cdot 6\text{H}_2\text{O}$, 13 mg/L $\text{CuCl}_2 \cdot 2\text{H}_2\text{O}$, 1.6 mg/L $\text{MnCl}_2 \cdot 2\text{H}_2\text{O}$ and 10 mg/L H_3BO_3 dissolved in water (33, 34). Trace element solution was added to a concentration of 1X to decrease variability due to metal content in water.

The following media are also used in this study: (i) M9+glycerol medium, which is identical to M9+glucose except with 1% glycerol substituted for 1% glucose; (ii) MOPS EZ Rich medium, which is a commercially available defined medium (Teknova, Cat. No. M2105); (iii) Low Salt (0.5g/l NaCl) LB Lennox (LB) medium (; (iv) Low Salt LB supplemented with 1% glucose (LB + glucose).

Adaptive evolution:

For adaptive evolution, ancestral strains were streaked on LB agar plates, and colonies were used to inoculate 14 independent 1 mL culture volumes in glucose minimal media. Cells were typically passaged during late exponential phase at a dilution of 1:1,000 in 1 mL culture volumes incubated in deep 96-well plates at 34 C and 400 rpm. The dilution and passaging rate varied with the strains' growth, meaning that strains were initially diluted between 1:100 and 1:500 once per day (~7-9 generations per day), and then gradually ramped up to a maximum passaging rate of two 1:1,000 dilutions each day (~20 $[\log_2(2,000)]$ generations per day as their fitness increased.

Sequencing library preparation:

After evolution, two clones were isolated from each population for genomic DNA purification and for next-generation sequencing using an adapted form of the Illumina transposase library preparation (35). Barcoded libraries were pooled and run in an Illumina HiSeq 2500.

Genome resequencing and analysis:

Genome resequencing and analysis was performed in parallel with two analytical pipelines to focus on multiply-mutated genes or on individual single nucleotide polymorphisms (SNPs). These analyses were conducted respectively (i) using Millstone (36) and Python scripting; or (ii) using a group of widely-distributed sequence-analysis tools and Python scripting. (i) Millstone is a custom software suite built by our lab for the purpose of whole genome mutational analysis. Illumina reads are aligned to a reference genome (NC_000913.3), and a list of variants is output that was then analyzed with custom scripting in Python 3.7. Code-base is available online at <http://churchlab.github.io/C321evolve/>. In brief, variants were culled based on minimum read depth and allele frequencies, multiply-hit genes were identified, cross-contamination events were sorted out, and a final list of genes was assembled that saw at least three unique mutational episodes in any of the four strains. (ii) A custom analytics pipeline was run in parallel to the Millstone analysis, using bowtie2 version 2.1.0 (37) to align reads to the reference genome and Picard version 1.44 to mark duplicate reads. A permissive list of candidate SNPs and indels was generated by applying the GATK UnifiedGenotyper (38) version 2.3 to all samples at once, with the minimum phred-scaled confidence threshold set to its most permissive value, 4.0. The list of candidate mutations was then filtered by excluding all sites with more than one alternate allele and all indels longer than one base pair because these sites are less likely to contain true variants and harder to call confidently. To ensure adequate coverage, it was required that the site: (1) have an average coverage depth of at least 10x across samples, (2) have zero coverage depth in no more than one sample, and (3) have at least ten total reads supporting the alternate allele. Because the samples are haploid, we required the alternate allele to be supported by at least 85% of the reads in at least one sample. Finally, read were filtered on GATK's quality score and strand bias fields (requiring QUAL > 50 and FS < 40).

Gene ontology analysis:

The gene ontology (GO) of all mutations was analyzed with reference to a set of standard categorizations for *E. coli* (39).

Neutral mutation rate analysis:

We briefly investigated whether faster adaptation of less-fit strains could be due to an elevated mutation rate. If this were the case, we would expect the C321 lineages to have an elevated mutation rate compared to the

ECNR2 lineages. According to theory, the number of *neutral* mutations in a clone relative to its ancestor is Poisson distributed with mean equal to the neutral mutation rate times the number of generations. In order to use this Poisson model, we have to restrict ourselves to independently-evolved clones, i.e. clones whose most recent common ancestor is the ancestor of all strains. This means that we (1) can use no more than one clone per population, and (2) can use no more than one clone per set of populations that are connected by cross-contamination/re-seeding events.

With these considerations, we selected six clones from the C321 (C) populations and six clones from the ancestral ECNR2 (E) populations according to the following rules. Using the maximum parsimony tree, we identified all clades supported by more than one mutation, as well as one C clade supported by a single prfB mutation. Then, within each of these clades, we picked the clone whose ID comes first in alphanumeric order. This ensures that we picked clones at random with respect to how many mutations they had. For each of these twelve clones, we then counted the number of single-hit synonymous mutations along the lineage from Generation 0 to the clone. The clones and mutation counts are included below.

Adding the counts of synonymous mutations from the clones from each lineage, we count 64 mutations per clone per 6K generations in the ECNR2 lineage and 78 mutations per clone per 6K generations in the C321 lineage. If synonymous mutations accumulate as a Poisson process average rate of 71 mutations per clone per 6K generations, we'd expect the difference between the counts in the two lineages to have a standard deviation of ~12 mutations, compared to an observed difference of 14 mutations. This suggests, that the data is consistent with the hypothesis that the two lineages are accumulating synonymous mutations at the same rate.

Clone	Synonymous mutations
C-A4-1	13
C-B3-1	12
C-C3-1	18
C-D4-1	10
C-E4-1	14
C-F3-1	11
E-A1-1	11
E-A2-1	14

E-C1-1	7
E-F1-1	11
E-G1-1	7
E-H1-1	14

Stop codon analysis:

To account for all possible stop codon changes, we considered three potential events: (i) direct conversion from one stop codon to another; (ii) read-through effects of mutating a stop codon into a sense codon; and, (iii) frameshift mutations close to the end of a protein-coding gene which would have the effect of switching termination from the wild-type stop codon to a new position. We only considered frameshift mutations that both occurred within 100bp (~33 amino acids (AA)) of the 3' end of a gene and that did not add more than 200bp (~66 AA) of additional length to the end of a gene. Based on our observations, we decided to exclude certain stop codons from further analysis because of when or where they occurred. We saw only three instances of direct UAA to UAG reversions: to *hemA* in C321 during the re-introduction of *prfA* to the strain in preparation for long-term passaging, and to the pseudogenes *eaeH* and *yehE* during passaging of the C321 (*prfA*+) and C321.ΔA-v2 lineages. We exclude these two latter reversions from our downstream analysis because they both occur in pseudogenes, and so are unlikely to be of great significance. Using the broader criteria described above, we catalogue 39 unique instances of stop codon changes (**Table S1**). Three changes are excluded from further analysis because they occur in pseudogenes, and five changes to *rph* and one to *wzzE* are ignored because they are either direct or indirect repairs of prior frameshift mutations occurring in either the wild-type K-12 strain, in the case of *rph*, or the C321 ancestor during *prfA* re-introduction, in the case of *wzzE*. This leaves 30 total termination codon changes, 9 of which are due to a point mutation to the termination codon itself, and 21 of which are due to frameshift mutations.

Analysis of parallel evolution:

Because there were several cross-contamination events between wells over the course of the evolution, we used phylogenetic methods to estimate the number of independent occurrences of each mutation. A sequence

alignment of all single base pair substitutions in all samples was constructed, and from this we found the maximum parsimony sample genealogy using MEGA7 version 7.0.16 (40) (**Fig. S11**). This genealogy was then used to identify the minimum number of distinct mutational events required to explain each sample genotype. This method is conservative with regard to identifying parallel evolution because the maximum parsimony genealogy may incorrectly group populations that acquired the same mutations into clades. Table S4 shows the mutations that we infer occurred more than one time within the c321 and/or c321-v2 populations, but which we did not observe in the ECNR2 populations. To identify parallel evolution at a higher level of biological organization, we counted the number of independent mutational events in genes in each GO process category. Table S5 shows the number of non-synonymous mutations in each GO category for populations descended from each of the c321, c321-v2, and ECNR2.

Allele reconstructions:

MAGE was used to reconstruct mutations of interest in the ancestral strains. Saturated overnight cultures were diluted 100-fold into 3 mL LB containing appropriate antibiotics and grown at 34 °C until mid-log. The integrated Lambda Red cassette in C321.ΔA derived strains was induced in a shaking water bath (42 °C, 300 rpm, 15 minutes), followed by incubation on ice for at least two minutes. The cells were then made electrocompetent at 4 °C by pelleting 1 mL of culture (16,000x rcf, 20 seconds) and washing twice with 1 mL ice cold deionized water (dH₂O). Electrocompetent pellets were resuspended in 50 μL of dH₂O containing the desired DNA. For MAGE oligonucleotides, 5 μM of each oligonucleotide was used. Please see Table 2 for a list of all oligonucleotides used in this study. For integration of dsDNA cassettes, 50 ng was used. Allele-specific colony PCR was used to identify desired colonies as previously described (41). Colony PCR was performed using Kapa 2G Fast HotStart ReadyMix following manufacturer protocols and Sanger sequencing was performed by Genewiz to verify strain engineering.

Doubling time measurement:

To assess fitness by measuring doubling times, strains were grown in triplicate in transparent flat-bottom 96-well plates (150 μL, 34 °C, 300 rpm). Kinetic growth (OD₆₀₀) was monitored on Eon plate readers at 5 minute intervals. After blanking reads by subtracting wells containing only media, doubling times were calculated by t_{double}

= $C \cdot \ln(2)/M$, where $C = 5$ minutes per time point and M is the maximum slope of $\ln(\text{OD}_{600})$. The slope was calculated based on the linear regression of $\ln(\text{OD}_{600})$ through 21 contiguous time points (60 minutes).

Head-to-head competition assays:

Fitness was also evaluated using head-to-head competition assays featuring a fluorescent reference strain. To construct the fluorescent reference strain we transformed wild-type MG1655 with a pET-plasmid vector containing mCardinal (42) under control of a strong synthetic promoter (Anderson: BBa_J23108). Competition assays were set up by growing cultures separately overnight, then mixing an equal amount of fluorescent reference strain with the strain whose fitness is to be measured at dilutions of 1:100 for both strains. This was done in plate-format, grown 24 hours in a shaker at 30°C / 300RPM, and assayed in a BD LT Fortessa flow cytometer, using the laser and filter settings for the Cy5 dye. The percentage of fluorescent cells was calculated after analysis in FloJo, and used as an inverse measurement of the fitness of the assayed strain.

nsAA incorporation assays:

We used the bipyridylalanine aminoacyl-tRNA synthetase (BipyARS) and *Methanococcus jannaschii* tRNA^{opt_{CUA}} as our OTS (43), which was recently shown to be more orthogonal to the native 20 amino acids than related engineered *M. jannaschii* tyrosyl-tRNA synthetase variants (44). As reporter proteins, we used ubiquitin fused N-terminally to super-folder GFP. The positive expression control contained no UAG sites (0-UAG), while the other second construct contained two UAG codons (2-UAG), the first between the two domains and the second internal to the GFP at position 151 (44). We measured GFP fluorescence normalized to culture optical density (FL/OD) in the presence and absence of p-Acetyl-phenylalanine (pAcF). To avoid catabolite repression of the arabinose inducible promoter system that regulates BipyARS, we used glycerol minimal media for these experiments.

Strains harboring GFP reporters and BipyARS/tRNA plasmids were inoculated from frozen stocks in biological triplicate and grown to confluence overnight in deep well plates. Experimental cultures were inoculated at 1:10 dilution in glycerol minimal media supplemented with chloramphenicol, arabinose, and pAcF. Cultures were incubated at 34 °C to an OD_{600} of 0.5–0.8 in a shaking plate incubator at 400 rpm (~3-4 h). GFP expression was

induced by addition of anhydrotetracycline, and cells were incubated at 34 °C for an additional 16-20 h before measurement.

Assays were performed in 96-well plate format. Cells were centrifuged at 5,000g for 3 min, washed with PBS, and resuspended in PBS after a second spin. GFP fluorescence was measured on a Biotek spectrophotometric plate reader using excitation and emission wavelengths of 485 and 525 nm (Gain = 80). Fluorescence signals were corrected for autofluorescence as a linear function of OD₆₀₀ using the parent C321.ΔA strain that does not contain a reporter. Fluorescence was then normalized by the OD₆₀₀ reading to obtain FL/OD.

SI Table 1. All mutations that affect stop codons.

Position	Occurrence	Type*	Gene	REF	ALT	Ancestral codon	New codon	Δ Tail length	Lineage**	Reason Excluded
115797	evolution	fs	hofB	CAAAAAG	CAAAAAG	TAA	TAG	-64	P-5-2	-
183606	C321 ancestor	fs	cdaR	GAT	GT	TAA	TAG	55	CFP	-
232548	evolution	p	yafE	A	G	TAA	TGA	0	P-12-1	-
315244	evolution	p	pseudogene	G	-	TAA	TAG	0	F-F6-1	pseudogene
474302	evolution	p	tesB	T	A	TAA	TGA	18	C-D4-1	-
578096	evolution	fs	rrrD	TGGGGGC	TGGGGGGC	TGA	TAG	460	E-E2-1	nonsense tail
635369	evolution	fs	ybdN	TCCCCCA	TCCCCCA	TAA	TAG	600	P-9-1 / C-A4-1 / C-A4-2	nonsense tail
675600	C321 ancestor	fs	ybeQ	CTG	CG	TAA	TGA	106	CFP	-
821493	evolution	fs	ybhM	GTTTTTTC	GTTTTTTC	TAG	TAA	32	E-B2-1	-
1006412	C321 ancestor	fs	zapC	TGG	TG	TAA	TGA	-61	CFP	-
1084580	evolution	fs	efeB	ATTTTTTG	ATTTTTTG	TAA	TAA	17	C-D3-1	no change
1189846	evolution	fs	phoP	ATTTTTTG	ATTTTTTG	TGA	ATC	931	C-C4-2 / F-B6-1	nonsense tail
1199759	evolution	fs	intE	GTTTTTG	GTTTTTG	TGA	TAA	-69	F-G5-2 / F-G5-1	-
1208533	C321 ancestor	fs	tfaE	TCA	TA	TAA	TAA	279	CFP	nonsense tail
1264970	prfA+ ancestor	p	hemA	G	-	TAA	TAG	0	P	-
1417538	evolution	fs	racC	CTTTTTTTC	CTTTTTTTC	TGA	TAA	-31	E-G1-1	-
1423525	evolution	fs	rzoR	TCCCCCG	CCCCCCG	TAA	TAA	0	P-13-1 / P-12-2 / P-3-1 / P-6-2	rzpR fix
1423525	prfA+ ancestor	fs	rzoR	TCCCCCG	TCCCCCCG	TAA	TAA	60	P	no change
1639535	evolution	fs	rrrQ	TCCCCCA	TCCCCCA	TGA	TAG	492	C-F3-2	nonsense tail
1655355	F11 ancestor	fs	ynfA	GCCCCCA	GCCCCA	TAA	TAA	23	F	no change
1660484	evolution	fs	ynfE	GAAAAAAT	GAAAAAAT	TAA	TAA	52	P-14-2	no change
1667344	evolution	p	mlc	T	C	TAA	TAG	0	E-F1-1	-
1757108	evolution	p	pykF	T	C	TAA	TAA	81	E-A2-1 / E-A2-2	no change
1757751	C321 ancestor	fs	ldtE	CTCTGGT	CT	TAA	TAG	80	CFP	-
1931971	evolution	fs	purT	TGGGGGT	TGGGGGGT	TAA	TGA	-52	F-D5-1 / F-D5-2 / F-G5-1 / F-G5-2	-
1967130	evolution	fs	cheY	GCCCCCG	GCCCCCG	TGA	TGA	-17	E-A2-1	no change
1968506	evolution	p	cheR	A	C	TAA	TGA	6	P-11-2	-
2024571	evolution	fs	rcsA	ATTTTIG	ATTTTIG	TAA	TGA	10	F-F6-2	-
2186661	evolution	fs	rcnA	GCCCCCT	GCCCCCT	TAA	TAA	559	F-C5-1	nonsense tail
2241812	evolution	p	yeiB	A	G	TAA	TAA	36	C-C4-1	no change
2297107	evolution	fs	ccmA	TCCCCCCT	TCCCCCCT	TGA	TGA	-48	F-E6-1	no change
2367984	evolution	fs	arnC	GCCCCCG	GCCCCCG	TAA	TGA	-4	P-11-2 / P-8-1 / E-F1-2	-
2370019	C321 ancestor	p	arnA	T	C	TGA	TAG	9	CFP	-
2770672	evolution	fs	ypjK	GAAAAAAT	GAAAAAAT	TAA	TAA	9	P-11-1	no change
2824495	C321 ancestor	fs	mltB	TGT	TT	TAA	TAA	66	CFP	no change
2984447	evolution	fs	yqeF	GCCCCCG	GCCCCG	TAG	TGA	-20	E-E1-1	-
3003473	evolution	fs	xdhB	CGGGGGGA	CGGGGGGA	TGA	TAA	476	C-B3-1 / P-13-2	nonsense tail
3019150	evolution	fs	ygfK	GAG	GAAG	TAA	CGC	994	C-D4-2	nonsense tail
3092826	evolution	p	gshB	T	C	TAA	TGA	36	C-G4-2 / C-E4-1	-
3134810	C321 ancestor	fs	yghT	GTG	GG	TAA	TAA	50	CFP	no change
3269600	evolution	p	yhaC	T	C	TAG	TAA	6	E-G1-1	-
3330353	C321 ancestor	fs	dacB	GTT	GTTT	TAA	TGA	-37	CFP	-
3365664	evolution	p	pseudogene	G	-	TAA	TAG	0	P-5-1 / P-8-2	pseudogene

3411546	evolution	fs	fis	GAAAAAAT	GAAAAAAT	TAA	TGA	-6	C-G3-2 / C-F3-1 / C-G3-1 / C-F3-2']	-
3411565	evolution	p	fis	T	C	TAA	TGA	102	C-B3-2 / C-B3-1 / C-D3-2 / C-D3-1	-
3418135	evolution	p	acrF	T	C	TAA	TAA	63	E-H2-2	no change
3598557	C321 ancestor	p	livJ	A	G	TAA	TAA	39	CFP	no change
3799382	evolution	fs	waaZ	ATTTTTTTC	ATTTTTTTC	TAA	TAA	90	F-G6-2 / P-12-2 / F-G6-1 / P-3-2	no change
3815879	evolution	fs	pseudogene	TCC	TCCC	TAA	TGA	28	C-G4-1 / C-G4-2 / P-14-1 / P-10-2 / C-E4-1 / W72 / C-E4-2 / P-8-1 / W62 / P-4-2	rph fix
3815879	evolution	fs	pseudogene	TCC	TC	TAA	TAG	69	F-C6-2 / F-C6-1	rph fix
3815907	evolution	fs	pseudogene	GTA	GA	TAA	TAG	68	F-E6-1 / F-E6-2	rph fix
3815916	evolution	fs	pseudogene	CAT	CT	TAA	TAG	68	F-F5-2 / F-F5-1	rph fix
3815943	evolution	fs	pseudogene	TCC	TC	TAA	TAG	68	F-G5-1 / F-G5-2	rph fix
3862515	C321 ancestor	fs	pseudogene	GCC	GC	TAA	TGA	-8	CFP	pseudogene
3862523	C321 ancestor	fs	pseudogene	TGCC	TC	TAA	TAG	-2	CFP	redundant
3867032	evolution	fs	ibpA	GTTTTTTC	GTTTTTTC	TAA	TAA	6	C-F4-2	no change
3902308	evolution	fs	bglB	ATTTTTTTTA	ATTTTTTTTA	TAA	TAA	39	E-B2-2 / F-B6-2	no change
3938217	evolution	fs	rbsK	GAG	GAAG	TGA	TAA	75	C-C3-2 / C-C3-1 / C-E3-1 / C-E3-2	-
3950463	evolution	fs	ilvX	CGGGGGT	CGGGGT	TAA	TAA	-67	E-C1-2 / E-C1-1	no change
3950463	evolution	fs	ilvX	CGGGGGT	CGGGGGTT	TAA	TGA	-79	E-F1-2 / E-E1-2	-
3970026	evolution	fs	wzzE	CGGGGGGC	CGGGGGGGGC	TGA	TGA	-39	P-13-1 / P-4-2 / P-1-2 / F-H5-1 / C-E4-1	wzzE fix
3970026	evolution	fs	wzzE	CGGGGGGC	CGGGGGGGGGGC	TGA	TGA	-36	C-C3-2 / C-C3-1	wzzE fix
3970026	evolution	fs	wzzE	CGGGGGGC	CGGGGGGGGGGC	TGA	TGA	21	C-E3-1 / C-E3-2	wzzE fix
3970026	evolution	fs	wzzE	CGGGGGGC	-	TGA	TAG	0	C-E4-2	wzzE fix
3970026	C321 ancestor	fs	wzzE	CGGGGGGC	CGGGGGGGGC	TAA	TGA	18	CFP	-
3980619	evolution	fs	wecG	CTT	CT	TGA	TAA	82	P-14-2	-
4293099	evolution	fs	nrfE	TGGGGGGGA	TGGGGGGGA	TAA	TGA	-2	E-E1-2 / P-6-2	-
4415881	evolution	fs	aidB	CGGGGGGA	CGGGGGGA	TAA	TGA	14	P-2-1 / E-A1-1 / E-A1-2 / P-11-2	-
4424542	C321 ancestor	fs	yjfy	GCA	GA	TAA	TAA	143	CFP	no change

4447866	C321 ancestor	fs	tamB	ATT	AT	TAA	TAA	95	CFP	no change
4472418	evolution	fs	pyrL	CAAAAAAAG	CAAAAAAAG	TAA	TAA	42	P-9-1 / C-D4-2 / P-7-2 / P-12-1	no change
4488572	evolution	fs	yjgR	TCCCCCCA	TCCCCCCA	TAA	TGA	24	P-13-2 / E-F1-1 / F-C6-1	-
4619469	C321 ancestor	fs	deoA	LONG:11bp	CG	TAA	TAA	-10	CFP	no change

* fs = frameshift; p = point mutation

** C = c321.ΔA; P = c321; E = ECNR2.1; F = c321.ΔA-v2

SI Table 2. All observed mutations to release factors *prfB* and *prfC*.

Position	Lineage	REF	ALT	Read Depth	Allele Frequency	Gene	Amino Acid change
3035437	E-H2-2	T	C	77.0	0.97	prfB	p.Lys282Arg/c.845A>G
3035437	E-H2-1	T	C	49.0	0.98	prfB	p.Lys282Arg/c.845A>G
3035546	C-D4-1	T	C	60.0	1.0	prfB	p.Thr246Ala/c.736A>G
3035546	C-C4-1	T	C	73.0	1.0	prfB	p.Thr246Ala/c.736A>G
3035546	C-B3-1	T	C	99.0	1.0	prfB	p.Thr246Ala/c.736A>G
3035546	C-B4-1	T	C	77.0	1.0	prfB	p.Thr246Ala/c.736A>G
3035546	C-C4-2	T	C	82.0	1.0	prfB	p.Thr246Ala/c.736A>G
3035546	C-B4-2	T	C	87.0	1.0	prfB	p.Thr246Ala/c.736A>G
3035546	C-D3-2	T	C	43.0	0.98	prfB	p.Thr246Ala/c.736A>G
3035546	C-B3-2	T	C	52.0	1.0	prfB	p.Thr246Ala/c.736A>G
3035546	C-D3-1	T	C	41.0	1.0	prfB	p.Thr246Ala/c.736A>G
3035774	C-F4-1	C	T	7.0	1.0	prfB	p.Glu170Lys/c.508G>A
3035774	C-A4-1	C	T	44.0	1.0	prfB	p.Glu170Lys/c.508G>A
3035774	C-D4-2	C	T	61.0	0.98	prfB	p.Glu170Lys/c.508G>A
3035774	C-F4-2	C	T	37.0	1.0	prfB	p.Glu170Lys/c.508G>A
3035774	C-A4-2	C	T	46.0	0.98	prfB	p.Glu170Lys/c.508G>A
3035546	F-G5-1	T	C	73.0	1.0	prfB	p.Thr246Ala/c.736A>G
3035546	F-E6-2	T	C	75.0	1.0	prfB	p.Thr246Ala/c.736A>G
3035546	F-D6-1	T	C	84.0	1.0	prfB	p.Thr246Ala/c.736A>G
3035546	F-D5-1	T	C	56.0	1.0	prfB	p.Thr246Ala/c.736A>G
3035546	F-D5-2	T	C	66.0	1.0	prfB	p.Thr246Ala/c.736A>G
3035546	F-F5-2	T	C	34.0	1.0	prfB	p.Thr246Ala/c.736A>G
3035546	F-E5-2	T	C	51.0	1.0	prfB	p.Thr246Ala/c.736A>G
3035546	F-B5-1	T	C	36.0	1.0	prfB	p.Thr246Ala/c.736A>G
3035546	F-G6-2	T	C	29.0	1.0	prfB	p.Thr246Ala/c.736A>G
3035546	F-F6-1	T	C	90.0	1.0	prfB	p.Thr246Ala/c.736A>G
3035546	F-F5-1	T	C	75.0	1.0	prfB	p.Thr246Ala/c.736A>G
3035546	F-B6-2	T	C	65.0	1.0	prfB	p.Thr246Ala/c.736A>G
3035546	F-G5-2	T	C	70.0	1.0	prfB	p.Thr246Ala/c.736A>G
3035546	F-B6-1	T	C	45.0	1.0	prfB	p.Thr246Ala/c.736A>G
3035546	F-C6-2	T	C	115.0	1.0	prfB	p.Thr246Ala/c.736A>G
3035546	F-F6-2	T	C	75.0	1.0	prfB	p.Thr246Ala/c.736A>G
3035546	F-C6-1	T	C	61.0	1.0	prfB	p.Thr246Ala/c.736A>G
3035546	F-B5-2	T	C	46.0	1.0	prfB	p.Thr246Ala/c.736A>G
3035546	F-E5-1	T	C	60.0	1.0	prfB	p.Thr246Ala/c.736A>G
3035546	F-D6-2	T	C	94.0	1.0	prfB	p.Thr246Ala/c.736A>G
3035546	F-G6-1	T	C	90.0	1.0	prfB	p.Thr246Ala/c.736A>G
3035546	F-E6-1	T	C	89.0	1.0	prfB	p.Thr246Ala/c.736A>G
4610462	F-C5-1	C	T	40.0	0.98	prfC	p.Ala350Val/c.1049C>T
4610462	F-C5-2	C	T	84.0	0.94	prfC	p.Ala350Val/c.1049C>T
4610477	F-F6-2	A	G	46.0	1.0	prfC	p.His355Arg/c.1064A>G
4610816	F-B6-2	T	C	82.0	1.0	prfC	p.Val468Ala/c.1403T>C
4610816	F-B6-1	T	C	55.0	1.0	prfC	p.Val468Ala/c.1403T>C

SI Table 3 - Summary of the most frequently-mutated genes in each evolved population. Only genes for which at least four instances are observed from any given starting population, or for which at least six instances are observed across all populations, are shown in this table.

Gene	Gene Length (bp)	Instances of mutation to evolved lineages					Brief Remarks	Previously Observed in ALE
		ECNR2	C321	C321.ΔA	C321.ΔA-v2	Total		
<i>aceE</i>	2,664	-	1	5	1	7		
<i>cyaA</i>	2,547	-	2	2	2	6		
<i>fdnG</i>	3,048	-	-	4	-	4		
<i>fimH</i>	903	1	1	2	11	15	Important for biofilm formation in M9 + glucose and LB	¶
<i>fis</i>	297	-	4	6	-	10		*
<i>flu</i>	3,120	14	-	5	13	32	Important for biofilm formation in M9 + glucose but not in LB	
<i>folA</i>	480	-	10	5	2	17	Hitchhiker mutation to promoter during C321 recoding	
<i>folM</i>	723	-	4	1	-	5		
<i>glrR</i>	1,335	-	4	-	-	4		
<i>gltB</i>	4,461	-	4	3	-	7	Highly expressed in biofilms in Gram-negative bacteria	*
<i>hyfB</i>	2,019	3	1	-	2	6		
<i>insH1</i>	1,017	2	2	3	1	8		
<i>kup</i>	1,869	1	4	2	-	7		*
<i>leuP</i>	87	4	1	6	4	15	Long strings of guanines were mutated in these tRNAs, a type of mutation that is a commonly found in mutS- hypermutator strains.	
<i>leuQ</i>	87	2	-	3	3	8		
<i>leuV</i>	87	5	-	-	4	9		
<i>mdtJ</i>	366	-	-	1	4	5	Knockout led to increased biofilm mass in minimal media	
<i>ompT</i>	954	5	1	-	1	7	Highly expressed in biofilms in Gram-negative bacteria	
<i>oxyR</i>	918	-	-	5	12	17	Null mutation upregulates <i>flu</i>	
<i>phoP</i>	672	4	-	1	6	11		
<i>prfB</i>	1,099	1	-	6	7	14	Release factor 2, discussed in text	
<i>prfC</i>	1,590	-	-	3	3	6	Release factor 3, discussed in text	
<i>pta</i>	2,145	-	5	1	-	6		
<i>ptrB</i>	2,061	3	1	2	-	6		
<i>ptsP</i>	2,247	2	2	1	2	7		
<i>purL</i>	3,888	1	4	2	-	7	Purine biosynthesis, specifically <i>purL</i> and <i>purT</i> , are important for biofilm formation in many Gram-negative bacteria	
<i>purT</i>	1,179	-	3	1	7	11		
<i>pykF</i>	1,413	9	4	1	2	16		*,§
<i>pyrC</i>	1,047	4	1	-	-	5		
<i>pyrE</i>	642	16	7	6	8	37	Mutation in MG1655 founder strain	†,‡,§
<i>rcsD</i>	2,673	2	-	1	3	6		
<i>rhcC</i>	4,194	2	2	-	3	7		
<i>rlmB</i>	732	3	3	1	3	10		
<i>rph</i>	717	2	4	2	8	16	Mutation in MG1655 founder strain	†,‡,§
<i>rpoB</i>	4,029	7	5	2	-	14	Commonly seen in adaptation to minimal media	†,‡,§
<i>rpoC</i>	4,224	10	7	4	2	23	Commonly seen in adaptation to minimal media	†,‡
<i>rsxC</i>	2,223	1	7	-	2	10		
<i>speA</i>	1,977	1	1	2	2	6		
<i>tktA</i>	1,992	2	1	2	1	6		
<i>xdhA</i>	2,259	3	1	1	2	7		
<i>yccS</i>	2,154	2	5	3	-	10		
<i>ycgB</i>	1,533	-	1	4	-	5		
<i>ydbA</i>	8,622	1	2	2	1	6		
<i>ydfJ</i>	1,368	1	-	4	1	6		
<i>yeeJ</i>	7,077	-	-	4	3	7		
<i>yegE</i>	3,318	2	4	-	-	6		
<i>yehB</i>	2,481	1	-	4	-	5		
<i>yfhM</i>	4,962	2	4	1	1	8		
<i>yfiH</i>	732	4	3	5	-	12		
<i>yneO</i>	5,323	-	4	2	-	6		

* Barrick et al.; † Conrad et al.; ‡ Herring et al.; § LaCroix et al.; || Monk et al.; ¶ Aguilar et al.

SI Table 4. SNPs seen in more than one independent recoded lineage missing *prfA*, but not found in ECNR2 lineages. C-lineages refer to C321.ΔA, F-lineages refer to C321.ΔA-v2.

Position	Ref	Alt	Independent origins	Clades	Gene	Amino acid change
40229	A	G	2	(C-E4-1;C-E4-2;C-G4-1;C-G4-2);(F-A6-1;F-A6-2)	caiA	NA
49768	A	G	2	(C-A4-1;C-A4-2);(F-B5-1;F-B5-2;F-B6-1;F-B6-2;F-C6-1;F-C6-2;F-H5-1;F-H5-2)	NA	NA
107375	GT	G	2	(C-D4-1);(F-A6-1;F-A6-2)	NA	NA
224738	G	A	2	(F-F5-1);(F-E6-2)	rrsH	NA
716166	A	AG	2	(C-D3-2);(C-G4-2)	potE	frameshift
875520	GC	G	2	(C-G3-1;C-G3-2);(F-C6-1)	gsiA	frameshift
1196946	A	AT	2	(C-C4-2);(F-B6-1)	phoP	frameshift
1243369	A	AG	2	(C-B3-1;C-B3-2;C-D3-1;C-D3-2);(C-D4-2;C-F4-2)	ycgB	frameshift
1270725	A	AG	2	(C-F3-2);(C-A4-1;C-A4-2)	NA	NA
1425603	A	AG	2	(F-D6-1;F-D6-2);(F-E5-1;F-E5-2)	ydaT	frameshift
1678153	A	AT	2	(C-F3-1;C-F3-2);(F-G5-1;F-G5-2)	mdtJ	frameshift
1678604	T	C	2	(C-G3-1;C-G3-2);(F-H5-1)	NA	NA
1936778	T	TG	2	(F-D5-1;F-D5-2);(F-G5-1;F-G5-2)	purT	frameshift
2048923	G	A	2	(C-G3-1;C-G3-2);(F-H5-2)	yeeJ	NA
2382800	T	TC	2	(C-B3-1);(F-C5-2)	menD	frameshift
2771523	T	TC	2	(F-H5-2);(F-G5-2)	NA	NA
3001978	A	AG	2	(C-D3-1);(F-B6-1;F-B6-2)	ygeR	frameshift
3037849	T	C	8	(C-B3-1;C-B3-2;C-B4-1;C-B4-2;C-C4-1;C-C4-2;C-D3-1;C-D3-2);(C-D4-1);(F-F6-1;F-F6-2);(F-B5-1;F-B5-2;F-B6-1;F-B6-2);(F-C6-1;F-C6-2);(F-D6-1;F-D6-2);(F-D5-1;F-D5-2);(F-E5-1;F-E5-2;F-E6-1;F-E6-2;F-F5-1;F-F5-2;F-G5-1;F-G5-2;F-G6-1;F-G6-2)	prfB	T->A
3038077	C	T	2	(C-A4-1;C-A4-2);(C-D4-2;C-F4-2)	prfB	E->K
3410910	C	CA	2	(C-E4-1;C-G4-2);(F-C6-1;F-C6-2)	NA	NA
3762046	A	AG	3	(C-B3-1;C-B3-2;C-B4-1;C-B4-2;C-C4-1;C-C4-2;C-D3-1;C-D3-2);(C-A4-1;C-A4-2;C-C3-1;C-C3-2;C-E3-1;C-E3-2;C-F3-1;C-F3-2;C-G0;C-G3-1;C-G3-2);(C-D4-1;C-D4-2;C-E4-1;C-E4-2;C-F4-2;C-G4-1;C-G4-2)	selA	frameshift
3817740	A	G	3	(C-B4-1;C-B4-2;C-C4-1;C-C4-2);(F-D5-1;F-D5-2);(F-E5-1;F-E5-2)	rph	NA
3817764	A	G	2	(F-F6-1;F-F6-2);(F-G6-1;F-G6-2)	rph	NA
3924987	G	A	2	(F-B6-1;F-B6-2);(F-H5-1;F-H5-2)	rsmG	A->V
3967466	CT	C	2	(F-A6-1;F-A6-2);(F-F5-1)	rhIB	frameshift
4096334	T	G	2	(C-B3-1;C-B3-2;C-D3-1;C-D3-2);(F-E5-1;F-E5-2)	NA	NA
4160505	A	G	2	(F-B5-1;F-B5-2);(F-G5-1;F-G5-2)	oxyR	S->G
4160511	C	T	2	(C-F4-2);(F-F6-1;F-F6-2)	oxyR	Q->*
4160536	T	C	2	(F-H5-2);(F-F5-1)	oxyR	L->P
4160969	AG	A	2	(F-D5-2);(F-E5-1;F-E5-2)	oxyR	frameshift
4160973	GA	G	2	(F-D5-1;F-D5-2);(F-E5-1)	oxyR	frameshift
4550911	G	A	2	(F-F5-1);(F-E6-1;F-E6-2)	fimH	C->Y
4550965	C	T	2	(C-C4-1;C-C4-2);(F-D6-1;F-D6-2)	fimH	S->L
4550971	A	G	2	(F-A6-1;F-A6-2);(F-E5-1;F-E5-2)	fimH	Y->C
4612372	C	T	2	(C-E4-1);(F-C5-1;F-C5-2)	prfC	A->V

SI Table 5. Gene ontology categorization of all mutations in the evolved poplatinos.

GO process description	GO process ID	C321 mutations	ECNR2 mutations	C321-v2 mutations	Fold increase in Recorded vs. Ecnr2
glycoprotein biosynthetic process	9101	2	1	12	7
DNA recombination	6310	11	1	1	6
tRNA aminoacylation for protein translation	6418	9	1	3	6
peptidoglycan biosynthetic process	9252	6	1	3	4.5
glutamate biosynthetic process	6537	5	1	2	3.5
regulation of transcription DNA-dependent	6355	8	2	5	3.25
translation	6412	12	4	12	3
amine catabolic process	9310	6	2	4	2.5
pyridoxine biosynthetic process	8615	4	1	1	2.5
polysaccharide catabolic process	272	2	1	3	2.5
asparagine biosynthetic process	6529	1	1	4	2.5
purine nucleotide biosynthetic process	6164	2	2	6	2
pentose-phosphate shunt non-oxidative branch	9052	3	1	1	2
DNA methylation	6306	1	1	3	2
O antigen biosynthetic process	9243	1	1	3	2
DNA-dependent DNA replication	6261	7	4	8	1.875
RNA catabolic process	6401	2	2	5	1.75
fatty acid oxidation	19395	6	3	4	1.667
flagellum assembly	9296	6	3	3	1.5
phosphorus metabolic process	6793	3	2	3	1.5
SOS response	9432	3	1	0	1.5
enterobacterial common antigen biosynthetic process	9246	2	1	1	1.5
nucleotide-sugar biosynthetic process	9226	2	1	1	1.5
betaine biosynthetic process	6578	1	1	2	1.5
response to temperature stimulus	9266	2	2	3	1.25
DNA repair	6281	3	3	4	1.167
taxis	42330	9	7	7	1.143
nitrogen compound metabolic process	6807	5	4	4	1.125
None	NA	239	232	236	1.024
carbohydrate catabolic process	16052	41	40	40	1.013
response to osmotic stress	6970	5	4	3	1
cytochrome complex assembly	17004	3	4	5	1
polyamine biosynthetic process	6596	4	3	2	1
methionine biosynthetic process	9086	3	2	1	1
ATP synthesis coupled proton transport	15986	3	2	1	1
amino sugar biosynthetic process	46349	3	2	1	1
tryptophan biosynthetic process	162	0	2	4	1
glycolate metabolic process	9441	2	1	0	1
aspartate biosynthetic process	6532	1	1	1	1
glyoxylate cycle	6097	0	1	2	1
RNA modification	9451	5	6	6	0.917
phospholipid biosynthetic process	8654	3	3	2	0.833
protein folding	6457	9	14	14	0.822
transcription	6350	38	51	45	0.814
anaerobic respiration	9061	23	28	19	0.75
glucose metabolic process	6006	3	2	0	0.75
methylglyoxal metabolic process	9438	2	2	1	0.75
peptidoglycan metabolic process	270	2	2	1	0.75
thiamin biosynthetic process	9228	2	2	1	0.75
response to drug	42493	6	10	8	0.7
glycolysis	6096	7	9	5	0.667
xenobiotic metabolic process	6805	5	6	3	0.667
DNA catabolic process	6308	2	5	4	0.6
sulfur metabolic process	6790	6	7	2	0.571
nucleobase nucleoside and nucleotide interconversion	15949	4	10	7	0.55

cellular amino acid catabolic process	9063	9	14	6	0.536
aerobic respiration	9060	4	7	3	0.5
gluconeogenesis	6094	1	2	1	0.5
galactose metabolic process	6012	1	1	0	0.5
Mo-molybdopterin cofactor biosynthetic process	6777	1	1	0	0.5
K antigen biosynthetic process	9248	0	1	1	0.5
lipopolysaccharide biosynthetic process	9103	0	1	1	0.5
homoserine biosynthetic process	9090	0	1	1	0.5
glycerol metabolic process	6071	0	1	1	0.5
protein modification process	6464	6	22	14	0.455
colanic acid biosynthetic process	9242	3	7	2	0.357
tricarboxylic acid cycle	6099	3	7	2	0.357
NAD biosynthetic process	9435	2	6	2	0.333
pyrimidine nucleotide biosynthetic process	6221	1	3	1	0.333
fermentation	6113	5	17	6	0.324
glycine biosynthetic process	6545	1	2	0	0.25
purine ribonucleotide biosynthetic process	9152	1	2	0	0.25
proline biosynthetic process	6561	0	2	1	0.25
translational attenuation	9386	1	3	0	0.167
response to desiccation	9269	1	3	0	0.167
histidine biosynthetic process	105	0	3	0	0
response to starvation	42594	0	3	0	0
response to stress	6950	0	2	0	0
macromolecule catabolic process	9057	0	1	0	0
cellular amino acid metabolic process	6520	0	1	0	0
iron ion transport	6826	5	0	3	0
folic acid biosynthetic process	46656	4	0	3	0
enterobactin biosynthetic process	9239	3	0	1	0
glyoxylate catabolic process	9436	3	0	1	0
chorismate biosynthetic process	9423	1	0	3	0
lysine biosynthetic process via diaminopimelate	9089	1	0	3	0
acetyl-CoA biosynthetic process from pyruvate	6086	3	0	0	0
nonribosomal peptide biosynthetic process	19184	2	0	1	0
coenzyme A biosynthetic process	15937	2	0	1	0
alanine biosynthetic process	6523	2	0	1	0
lipopolysaccharide core region biosynthetic process	9244	1	0	2	0
response to radiation	9314	1	0	2	0
lipoprotein biosynthetic process	42158	1	0	2	0
leucine biosynthetic process	9098	1	0	2	0
glutathione biosynthetic process	6750	2	0	0	0
arginine biosynthetic process	6526	2	0	0	0
phosphoenolpyruvate-dependent sugar phosphotransferase system	9401	1	0	1	0
carnitine catabolic process	42413	1	0	1	0
lipid A biosynthetic process	9245	1	0	0	0
DNA metabolic process	6259	1	0	0	0
S-adenosylmethionine biosynthetic process	6556	1	0	0	0
lipoate biosynthetic process	9107	1	0	0	0
L-phenylalanine biosynthetic process	9094	1	0	0	0
coenzyme and prosthetic group biosynthetic process	46138	0	0	1	0
pentose-phosphate shunt oxidative branch	9051	0	0	1	0
putrescine catabolic process	9447	0	0	1	0
pyruvate catabolic process	42867	0	0	1	0
glutamine biosynthetic process	6542	0	0	1	0
putrescine transport	15847	0	0	1	0
biotin biosynthetic process	9102	0	0	1	0
cysteine biosynthetic process	19344	0	0	1	0
glucan biosynthetic process	9250	0	0	1	0
polysaccharide biosynthetic process	271	0	0	1	0
gamma-aminobutyric acid catabolic process	9450	0	0	1	0
pilus assembly	9297	0	0	1	0

SI Table 6. Oligonucleotides used in this study.

Oligo Name	Sequence
P_C321D_4102449	CCGGTTTTGCCAGACTCCG
P_C321D_1263523	GCAGATGACGCGCCACCG
P_C321D_1511492	CATATAGAGATCGCGCGGGGA
P_C321D_3092256	GCGCTATTGAATTGCTGATTAACA
P_C321D_3990077	AGATTGTATCGTTTGGTCTCGATCC
P_C321D_322579	GGATATGGCTCTATTATCCAGGGC
P_FIX_4102449	CCGGTTTTGCCAGACTCCA
P_FIX_1263523	GCAGATGACGCGCCACCA
P_FIX_1511492	CATATAGAGATCGCGCGGGG
P_FIX_3092256	GCGCTATTGAATTGCTGATTAACG
P_FIX_3990077	AGATTGTATCGTTTGGTCTCGATCT
P_FIX_322579	GGATATGGCTCTATTATCCAGGGT
P_COM_4102449	AGCAGTTCTCAATCCGATTCATTAAC
P_COM_1263523	AAATCTTCTCTGTCGCGAAAC
P_COM_1511492	ACGCAGGATTACATTGCCATTATG
P_COM_3092256	GGCGCTCAACAAAGGCAAA
P_COM_3990077	CGCGGTTATACAGATACCAACC
P_COM_322579	CTCACAGCGGTCAACATAAC
prfA-F	CAACCAACCAATGCTGTTG
prfA-R	GTCGCTTTCAGAAATGTG
prfA-gRNA1-F	CTTTTTTACAGGGTGGAGGGTTTTAGAGCTAGAAATAGCAAG
prfA-gRNA2-F	ACAGGGTGGAGGAGGAATAAGTTTTAGAGCTAGAAATAGCAAG
gRNA-seq-F	AGTAAGGCAGCGGTATCATC
MAGE_prfBT246A	G*C*AGATTTCGGTACGGTTAACGTGCTACCGCCCGCGGACGcGCGATAAACGTCAATGCGCAGATCCGC CGGGTTGATTCGATATCA
MAGE_prfBE170K	G*G*AGATTTTATCGTACGGATTAATACCCGCCACTTACCTTtCGACTCTTCGATGATTCAGTTTTGAAAC CACGCGATTCTGCCCA
MAGE_prfCA350V	G*G*ATATCGCCGGATACGCTTCTTCAACGTGCGAACGGTACCCaCCATAAAGGTCAGCGCGTCGGAGATCA CCACATCTTTCGAGTGC
asPCR-prfBT246A-mut-F	CGCATTGACGTTTATCGCG
asPCR-prfBT246A-WT-F	CGCATTGACGTTTATCGCA
asPCR-prfBE170K-mut-F	CTGAAATCATCGAAGAGTCTGA
asPCR-prfBE170K-WT-F	CTGAAATCATCGAAGAGTCTGG
asPCR-prfB-R	CTTCGCTTTCATCTGCTTC
asPCR-prfCA350V-mut-F	GCGCTGACCTTTATGGt
asPCR-prfCA350V-WT-F	GCGCTGACCTTTATGGC
asPCR-prfC-R	CTTCGGAAAGCTGTACCAAG
prfB-removeFS-F	ACGTTCTTAGGGGGTATCTTACTACGACGCCAAGAAAG
prfB-removeFS-R	CTCTTCTTGGCGTCTAGTCAAGATACCCCTAAGAAGCTC
prfB_vars-seq	GTATGTTCTTGGCGAATATG
prfC_vars-seq	GATACCCGTACCGTAGAAG
MAGE-KO-fis	A*A*ATTTTGCGTAAACAGAAATAAAGAGCTGACAGAACTATGTaatAAtgACGCGTAAATTTCTGACGACTGAC CGTTTCTACCGTAACT
MAGE-KO-mdtJ	A*C*CGGTAATTTCTGTAGCAATAGCCAGACCTAATAAAATCCatAtcaATACATTGCTCTTCTCTGCAAGAGA ATTATTTAATTTTCG
MAGE-KO-oxvR	C*C*GCACGCCGAAAATGGCGGTGTTCCAGCAATGCCACCAGtTatTatcaATCACGAATATTCATTATCCATCCT CCATCGCCACGATAGT
MAGE-KO-purT	A*C*ACACGCAAACGTTTTCTGTTTACTGCGCGCGGAATTAATCAGGGGATATTCGTTATGtaaTaATgAGGCA CTGCGCTGCGTCCGGCA
fimH_C65Y-MAGE	G*C*AGTGTGACATAGTCTGTAATGTTTCCGGATAATCGTTATGGTAAAAGATTGCGTCAAAGATCCACGA CCAGGTTTTGCCACAT
fimH_S83L-MAGE	A*T*TTTACGGTCCCGGAAAAATTAGATAACACGCGCCATAAGCCAAGCCTCGTTGCAGTGTGACATAGTCTG TAATGGTTTCCGGATAA
fimH_65-ASPCR-WT	GGATCTTTCGACGCAAATCTTTTG
fimH_65-ASPCR-mut	GGATCTTTCGACGCAAATCTTTTA
fimH_83-ASPCR-WT	GTCACACTGCAACGAGGCTC
fimH_83-ASPCR-mut	GTCACACTGCAACGAGGCTT
fimH-ASPCR-R	CTGCCACTATATTTACGGTCCC
fis-ASPCR-WT	GTAACAGAAATAAAGAGCTGACAGAACTATGTTC

fis-ASPCR-mut	GTAACAGAAATAAAGAGCTGACAGAACTATGTAA
foIA-ASPCR-WT	TCTCAATGATCAGTCTGATTGCGGCGTTAG
foIA-ASPCR-mut	TCTCAATGATCAGTCTGATTGCGGCGTAAT
mdtJ-ASPCR-WT	GTAATTTCTGTAGCAATAGCCAGACCTAATAAAATCCAA
mdtJ-ASPCR-mut	GTAATTTCTGTAGCAATAGCCAGACCTAATAAAATCCAT
oxyR-ASPCR-WT	GATGGAGGATGGATAATGAATATTCGTGATC
oxyR-ASPCR-mut	GATGGAGGATGGATAATGAATATTCGTGATT
purT-ASPCR-WT	CGGAATTAATCAGGGGATATTCGTTATGA
purT-ASPCR-mut	GGAATTAATCAGGGGATATTCGTTATGT
fis-ASPCR-R	GCAGCGTACCACGGTTGATGCC
foIA-ASPCR-R	CAGTCATCCGGCTCGTAATCCGGG
mdtJ-ASPCR-R	GACGATTTTAGGCCATTGAGCGTGATGATCG
oxyR-ASPCR-R	TGTTGCGCAGAGTTTCCAGGCTGG
purT-ASPCR-R	TAATGACATGGGAGCGATGCGCGA
pfoIA-ins-F	cttacattaattgcgttgccTTCCTCAACATCATCCTCGC
pfoIA-ins-R	gtggtgatggtgcatTGAGATTTCCCGATAAAAAAATTGTC
mCard-bbone-F	atgcacatcatcaccac

SI References

1. Conrad TM, et al. (2010) RNA polymerase mutants found through adaptive evolution reprogram *Escherichia coli* for optimal growth in minimal media. *Proc Natl Acad Sci U S A* 107(47):20500–5.
2. Herring CD, et al. (2006) Comparative genome sequencing of *Escherichia coli* allows observation of bacterial evolution on a laboratory timescale. *Nat Genet* 38(12):1406–1412.
3. LaCroix RA, et al. (2015) Use of adaptive laboratory evolution to discover key mutations enabling rapid growth of *Escherichia coli* K-12 MG1655 on glucose minimal medium. *Appl Environ Microbiol* 81(1):17–30.
4. Barrick JE, et al. (2009) Genome evolution and adaptation in a long-term experiment with *Escherichia coli*. *Nature* 461(7268):1243–1247.
5. Aguilar C, et al. (2012) Genetic changes during a laboratory adaptive evolution process that allowed fast growth in glucose to an *Escherichia coli* strain lacking the major glucose transport system. *BMC Genomics* 13. doi:10.1186/1471-2164-13-385.
6. Monk JW, et al. (2016) Rapid and Inexpensive Evaluation of Nonstandard Amino Acid Incorporation in *Escherichia coli*. *ACS Synth Biol* 6(1):45–54.
7. Jensen KF (1993) The *Escherichia coli* K-12 “wild types” W3110 and MG1655 have an *rph* frameshift mutation that leads to pyrimidine starvation due to low *pyrE* expression levels. *J Bacteriol* 175(11):3401–7.
8. Danese PN, Pratt LA, Dove SL, Kolter R (2000) The outer membrane protein, Antigen 43, mediates cell-to-cell interactions within *Escherichia coli* biofilms. *Mol Microbiol* 37(2):424–432.
9. Schembri MA, Kjaergaard K, Klemm P (2003) Global gene expression in *Escherichia coli* biofilms. *Mol Microbiol* 48(1):253–267.
10. Bay DC, Stremick CA, Slipski CJ, Turner RJ (2017) Secondary multidrug efflux pump mutants alter *Escherichia coli* biofilm growth in the presence of cationic antimicrobial compounds. *Res Microbiol* 168(3):208–221.
11. Bossi L (1983) Context effects: Translation of UAG codon by suppressor tRNA is affected by the sequence following UAG in the message. *J Mol Biol* 164(1):73–87.
12. Martin R, Weiner M, Gallant J (1988) Effects of release factor context at UAA codons in *Escherichia coli*. *J Bacteriol* 170(10):4714–7.
13. Poole ES, Brown CM, Tate WP (1995) The identity of the base following the stop codon determines the efficiency of in vivo translational termination in *Escherichia coli*. *EMBO J* 14(1):151–158.
14. Nakamura Y, Kawakami K, Mikuni O (1990) Alternative Translation and Functional Diversity of Release Factor 2 and Lysyl-tRNA Synthetase. *Post-Transcriptional Control of Gene Expression* (Springer Berlin Heidelberg, Berlin, Heidelberg), pp 455–464.
15. Brown CM, Stockwell PA, Trotman CNA, Tate WP (1990) The signal for the termination of protein synthesis in prokaryotes. *Nucleic Acids Res* 18(8):2079–2086.
16. Korkmaz G, Holm M, Wiens T, Sanyal S (2014) Comprehensive analysis of stop codon usage in bacteria and its correlation with release factor abundance. *J Biol Chem* 289(44):30334–42.
17. Keiler KC, Waller PRH, Sauer RT (1996) Role of a Peptide Tagging System in Degradation of Proteins Synthesized from Damaged Messenger RNA. *Science (80-)* 271(5251). Available at: <http://science.sciencemag.org/content/271/5251/990> [Accessed May 11, 2017].
18. Dulebohn D, Choy J, Sundermeier T, Okan N, Karzai AW (2007) Trans-Translation: The tmRNA-Mediated Surveillance Mechanism for Ribosome Rescue, Directed Protein Degradation, and Nonstop mRNA Decay.

Biochemistry 46(16):4681–4693.

19. Chadani Y, et al. (2010) Ribosome rescue by Escherichia coli ArfA (YhdL) in the absence of trans-translation system. *Mol Microbiol* 78(4):796–808.
20. James NR, Brown A, Gordiyenko Y, Ramakrishnan V (2016) Translational termination without a stop codon. *Science* (80-) 354(6318). Available at: <http://science.sciencemag.org.libproxy.mit.edu/content/354/6318/1437/tab-pdf> [Accessed March 27, 2017].
21. Yusupov MM, et al. (2001) Crystal Structure of the Ribosome at 5.5 Å Resolution. *Science* (80-) 292(5518). Available at: <http://science.sciencemag.org/content/292/5518/883> [Accessed May 11, 2017].
22. Ejby M, Sørensen MA, Pedersen S (2007) Pseudouridylation of helix 69 of 23S rRNA is necessary for an effective translation termination. *Proc Natl Acad Sci U S A* 104(49):19410–5.
23. O'Connor M, Gregory ST (2011) Inactivation of the RluD pseudouridine synthase has minimal effects on growth and ribosome function in wild-type Escherichia coli and Salmonella enterica. *J Bacteriol* 193(1):154–62.
24. Heurgue-Hamard V, Champ S, Engström A, Ehrenberg M, Buckingham RH (2002) The hemK gene in Escherichia coli encodes the N5-glutamine methyltransferase that modifies peptide release factors. *EMBO J* 21(4):769–778.
25. Nakahigashi K, et al. (2002) HemK, a class of protein methyl transferase with similarity to DNA methyl transferases, methylates polypeptide chain release factors, and hemK knockout induces defects in translational termination. *Proc Natl Acad Sci U S A* 99(3):1473–8.
26. Mora L, Heurgué-Hamard V, de Zamaroczy M, Kervestin S, Buckingham RH (2007) Methylation of Bacterial Release Factors RF1 and RF2 Is Required for Normal Translation Termination in Vivo. *J Biol Chem* 282(49):35638–35645.
27. SaiSree L, Reddy M, Gowrishankar J (2001) IS186 insertion at a hot spot in the lon promoter as a basis for lon protease deficiency of Escherichia coli B: identification of a consensus target sequence for IS186 transposition. *J Bacteriol* 183(23):6943–6.
28. Baneyx F, Georgiou G (1990) In vivo degradation of secreted fusion proteins by the Escherichia coli outer membrane protease OmpT. *J Bacteriol* 172(1):491–4.
29. Zilhão R, Cairrão F, Régnier P, Arraiano CM (1996) PNPase modulates RNase II expression in Escherichia coli: implications for mRNA decay and cell metabolism. *Mol Microbiol* 20(5):1033–1042.
30. Lopez PJ, Marchand I, Joyce SA, Dreyfus M (1999) The C-terminal half of RNase E, which organizes the Escherichia coli degradosome, participates in mRNA degradation but not rRNA processing in vivo. *Mol Microbiol* 33(1):188–199.
31. Michel-Reydellet N, Woodrow K, Swartz J (2005) Increasing PCR fragment stability and protein yields in a cell-free system with genetically modified Escherichia coli extracts. *J Mol Microbiol Biotechnol* 9(1):26–34.
32. Hong SH, et al. (2015) Improving Cell-Free Protein Synthesis through Genome Engineering of Escherichia coli Lacking Release Factor 1. *ChemBioChem* 16(5):844–853.
33. Brockman IM, Prather KLJ (2015) Dynamic knockdown of E. coli central metabolism for redirecting fluxes of primary metabolites. *Metab Eng* 28:104–113.
34. Kunjapur AM, Hyun JC, Prather KLJ (2016) Deregulation of S-adenosylmethionine biosynthesis and regeneration improves methylation in the E. coli de novo vanillin biosynthesis pathway. *Microb Cell Fact* 15(1):1.

35. Baym M, et al. (2015) Inexpensive Multiplexed Library Preparation for Megabase-Sized Genomes. *PLoS One* 10(5):e0128036.
36. Goodman DB, et al. (2017) Millstone: software for multiplex microbial genome analysis and engineering. *Genome Biol* 18(1):101.
37. Langmead B, Salzberg SL (2012) Fast gapped-read alignment with Bowtie 2. *Nat Methods* 9(4):357–9.
38. DePristo MA, et al. (2011) A framework for variation discovery and genotyping using next-generation DNA sequencing data. *Nat Genet* 43(5):491–8.
39. Riley M, et al. (2006) Escherichia coli K-12: a cooperatively developed annotation snapshot--2005. *Nucleic Acids Res* 34(1):1–9.
40. Kumar S, et al. (2016) MEGA7: Molecular Evolutionary Genetics Analysis Version 7.0 for Bigger Datasets. *Mol Biol Evol* 33(7):1870–1874.
41. Isaacs FJ, et al. (2011) Precise manipulation of chromosomes in vivo enables genome-wide codon replacement. *Science (80-)* 333(6040):348–353.
42. Chu J, et al. (2014) Non-invasive intravital imaging of cellular differentiation with a bright red-excitable fluorescent protein. *Nat Methods* 11(5):572–8.
43. Xie J, Liu W, Schultz PG (2007) A Genetically Encoded Bidentate, Metal-Binding Amino Acid. *Angew Chemie* 119(48):9399–9402.
44. Kunjapur AM, et al. (2017) Engineering post-translational proofreading to discriminate non-standard amino acids. *bioRxiv*. Available at: <http://www.biorxiv.org/content/early/2017/06/30/158246> [Accessed July 1, 2017].